

# Fabrication of eco-friendly superhydrophobic and superoleophilic PHB-SiO<sub>2</sub> bionanofiber membrane for gravity-driven oil/water separation

Fatma Bayram Sariipek<sup>1</sup>  | Yasemin Gündoğdu<sup>2,3</sup>  | Hamdi Şükür Kiliç<sup>3,4</sup> 

<sup>1</sup>Department of Chemical Engineering, Faculty of Engineering and Nature, Konya Technical University, Konya, Türkiye

<sup>2</sup>Department of Computer Technologies, Kadınhanı Faik İçil Vocational High School, Selçuk University, Konya, Türkiye

<sup>3</sup>Directorate of Laser Induced Proton Therapy Application and Research Center, Selçuk University, Konya, Türkiye

<sup>4</sup>Department of Physics, Faculty of Science, Selçuk University, Konya, Türkiye

## Correspondence

Hamdi Şükür Kiliç, Department of Physics, Faculty of Science, Selçuk University, Konya, Türkiye.  
Email: [hamdisukurkilig@selcuk.edu.tr](mailto:hamdisukurkilig@selcuk.edu.tr)

## Abstract

In this study, eco-friendly superhydrophobic (SH) and superoleophilic (SO) poly (3-hydroxybutyrate) (PHB)-SiO<sub>2</sub> bio-nanofiber membrane has been successfully fabricated for oil–water separation. Firstly, silica nanoparticles (SiNPs) have been synthesized via green laser ablation technique. It was placed into PHB matrix in different contents by controlling the time of ablation and then PHB-SiO<sub>2</sub> nanofibrous mats were obtained on commercial stainless-steel mesh with various mesh sizes by electrospinning method. The surface morphology and chemical structure of all obtained samples have been characterized by FT-IR, FE-SEM and HR-TEM techniques. It has been observed that SiNPs obtained within 30 min ablation time, with an average size distribution between 10 nm and 200 nm with spherical shape have been uniformly anchored on PHB nanofibers. PHB-SiO<sub>2</sub> fibrous membrane has shown superhydrophobicity with maximum water contact angle of 160.23° and superoleophilicity with oil contact angle (OCA) of being nearly 0° in air. Later, SH and SO membranes were directly employed for oil water separation without using any chemical reagent or additional force, and maximum efficiency of separation higher than 99% has been measured. These results has indicated that environmental friendly PHB-SiO<sub>2</sub> bio-nanofiber membrane offers high potential for using in gravity-driven oil–water separation.

## KEYWORDS

electrospinning, laser ablation, oil–water separation, PHB, SiNPs, superhydrophobic and superoleophilic surfaces

## 1 | INTRODUCTION

Concerns over oil spillage have grown in recent decades with increasing commerce of petroleum products in the globalized world. Catastrophic oil spillages resulted in industrial or transportation accidents, such as one in Mexico Gulf, remind us some urgent need to develop an eco-friendly, cost-efficient and large-scale solution to reduce damage to the marine and aquatic ecosystem.<sup>1,2</sup> Conventional remedies for dealing with

oil spillages include the use of adsorbents,<sup>3</sup> skimmers,<sup>4</sup> air flotation,<sup>5</sup> gravity sedimentation,<sup>6</sup> centrifugation,<sup>7</sup> coagulation/flocculation<sup>8</sup> and so on. These traditional separation techniques have a number of drawbacks such as poor selectivity, low separation efficiency, slow operation, high energy consumption and secondary contamination. As a result, developing an eco-friendly, selective, simple-to-apply and inexpensive technique for efficient oil–water separation is a critical and necessary application.

Biomimicry, that can be described as the imitation of natural elements, is a good way to create functional materials. In respect to wettable or non-wettable surfaces, it offers many models for some improvement on synthetic materials. For instance, various plants and animals with superhydrophobic surfaces in nature (such as lotus flower, butterfly wings, water spider legs) exhibit WCA values higher than  $150^\circ$  and slip angles lower than  $10^\circ$ .<sup>9,10</sup> Lately, for separation of oily mixtures, surfaces with superhydrophobic and superoleophilic features inspired by the lotus leaf have provided an alternative manner.<sup>11,12</sup> Because separating oil from water in oil–water mixtures is largely an interface event, all researchers attempt for designing superwettability surfaces via surface functionalization.<sup>13,14</sup> In theory, the wettability of a surface is influenced by its surface chemistry and roughness. The most effective way for selectively removing oil from oily water mixtures is to utilize a pierced or porous membrane constructed from a material with a surface energy between oil and water. Various investigations are conducted regarding superhydrophobic and/or superoleophilic surface modifications for oily separations. Mostly, superhydrophobic surfaces show superoleophobic properties due to their highly rough structure. Because these surfaces, in terms of surface energy, contain components that are similar to oil, and therefore are quite different from water. For creating the superhydrophobic and/or superoleophilic surfaces, low surface energy substances are either utilized to modify the surface of rough structures or a rough surface is constructed on the surface of low surface energy materials.<sup>15,16</sup> In the literature, many recent research on oil–water separation have focused upon the superhydrophobic-superoleophilic surface modifications of spongy substances.<sup>17–19</sup>

Membrane-based separation, an improved purification and separation technique, has widely employed for treatment of oily wastewater when compared to the traditional oil–water separation method because of its binary functions of preventing and adsorbing the filter supplies as well as the advantages of simple preparation and operation, excellent separation efficiency, high flexibility and outstanding anti-fouling feature.<sup>20,21</sup> The choice of substrate membrane material in the production of an ideal membrane material used for oily separations which is of great importance and recently, many studies for oil–water separation have concentrated on superhydrophobic-superoleophilic surface modifications of porous substrate materials including fabrics/textiles,<sup>22</sup> polymeric membranes,<sup>23</sup> sponges,<sup>24</sup> filter papers<sup>25</sup> and metal meshes.<sup>26,27</sup> The metallic mesh-based SH-SO membranes have greater mechanical strength and permeableness, as well as less pressure drop in comparison to the porous membranes. Stainless steel materials, one of the metallic mesh substrates, is commonly used as the base substrate and its wetting behavior can be adjusted to SH-SO condition through modification of surface chemistry and

morphology.<sup>19</sup> The SH-SO membrane materials prepared with a combination of stainless-steel mesh as a substrate and polymeric and/or inorganic material as a top layer have lately attracted a lot of attention from researchers due to their designability and processability. Many surface modification may be approached including dip coating,<sup>28</sup> spray-coating,<sup>29</sup> sol-gel,<sup>30</sup> atomic layer deposition,<sup>31</sup> self-assembly,<sup>32</sup> chemical vapor deposition<sup>33</sup> and electrospinning<sup>34</sup> and have been studied to produce separation membranes for oily wastewater treatment.

Electrospinning method has drawn a lot of interest in the last two decades because of its cost-efficiency, simplicity, high flexibility and porosity, large specific surface area and excellent separation performance.<sup>35</sup> Smooth continuous fibers having diameters ranging from roughly 1 mm to 10 nm can be fabricated from an electrified fluid by electrospinning. Nanofiber membranes developed to separate oil and water for the last 10 years have been widely employed because of their high selectivity and separation efficiency, environmental friendliness, simple separation processes and long-term reusability. For instance, Lee et al. have produced SH-SO polystyrene (PS) nanofiber membrane with high separation efficiency and found that diesel and water contact angles of deposited PS nanofibrous mats on the stainless steel meshes were  $0^\circ$  and  $155^\circ \pm 3^\circ$ , respectively. In another study, Wu et al. have developed a SH-SO poly(vinylidene fluoride) (PVDF) fibrous membrane and the manufactured PVDF nanofibrous membrane has displayed a WCA of  $152^\circ \pm 2^\circ$  and OCA of  $0^\circ$  in air and separation efficiency higher than 99%.<sup>36</sup> The electrospinning technology has highly been used to create nanofibers incorporating metal and metal oxide nanoparticles (NPs) for membrane separation applications. For example, Moatmed et al. have manufactured PS nanofibers modified with  $\text{Fe}_3\text{O}_4$  NPs to obtain a super-hydrophobic surface and the prepared  $\text{PS}@ \text{Fe}_3\text{O}_4$  10wt.% nanofibrous membrane with a WCA value of  $162^\circ$  exhibited highly separation efficiency of 99.8% and ultrahigh flux ( $5000 \text{ L m}^{-2} \text{ h}^{-1}$ ).<sup>37</sup> In another research, Ye et al. have fabricated polylactic acid (PLA) based nanofiber membranes by incorporating different metal oxides NPs ( $\text{SiO}_2$ ,  $\text{TiO}_2$ ,  $\text{Al}_2\text{O}_3$ , and  $\text{CeO}_2$ ) into PLA matrix by electrospinning to separate oil–water mixtures and as a result, they have shown that  $\text{SiO}_2$  modified PLA bionanofiber membranes with the highest WCA value of  $135 \pm 3^\circ$  exhibited high separation efficiency (up to 98.0%) and high separation flux ( $17,800 \text{ L m}^{-2} \text{ h}^{-1}$ ).<sup>38</sup> Jiang et al. have prepared PVDF- $\text{SiO}_2$  nanofibrous membranes with excellent separation performance of  $99 \pm 0.1\%$  and high separation flux of  $1857 \pm 101 \text{ L m}^{-2} \text{ h}^{-1}$  and observed that WCA values of the prepared nanofibrous membranes enhanced from  $138.5 \pm 1^\circ$  to  $150.0 \pm 1.5^\circ$  with increasing  $\text{SiO}_2$  content.<sup>39</sup> The effect of the content, size, and shape of the loaded

silica NPs on the roughness and chemistry of the resultant membrane surface have been clearly seen in many surfaces modification studies for the separation of oil-water mixtures.<sup>40–42</sup> SiO<sub>2</sub> NPs are highly utilized as functional fillers in many applications, especially hydrophobicity, thanks to their superior thermal and chemical stability, as well as their ability to be functionalized due to their silanol groups. Furthermore, SiO<sub>2</sub> NPs are inexpensive and readily available and are not harmful to the environment compared to fluorinated additives. Hydrophobic SiO<sub>2</sub> NPs with low surface energy that can be synthesized by various wet-chemistry processes such as sol-gel process,<sup>43</sup> modified stöber method<sup>44</sup> and surfactants<sup>45</sup> have utilized from many researchers for manufacturing a new membrane material. Lin et al. fabricated an electrospun PHB-PCL nanofiber substrate to be used in packaging applications and modified the nanofiber surface with SiO<sub>2</sub>-TiO<sub>2</sub> composite nanoparticles produced by the stöber method. It was observed that the prepared PCL-PHB/SiO<sub>2</sub>-TiO<sub>2</sub> composite membrane had excellent hydrophobicity and antibacterial activity with a water contact angle of 144° ± 1°.<sup>46</sup> In another study, PAN-SiO<sub>2</sub> nanofibers were produced to be used in the separation of oil-water emulsion mixtures. First, PAN nanofibers were produced and then the fibrous surface was modified with SiO<sub>2</sub> nanoparticles produced by the sol-gel method.<sup>47,59</sup> Conventional wet chemistry processes such as sol-gel, stöber etc., used to produce SiO<sub>2</sub> nanoparticles, are limited by their scalability, slow kinetics and batch operation, which typically results in an unpredictable variation in the physicochemical features of nanoparticles. Furthermore, chemical precursors used during nanoparticle synthesis can cause contamination on the obtained nanomaterial surfaces, and harmful residues as well as by-product wastes can be released into the environment.<sup>48</sup> Compared to chemical methods, physical methods have superior advantages in terms of regularity of nanoparticle production. In recent years, many physical techniques such as UV irradiation, lithography, UV irradiation, ultrasonic fields and laser ablation have been used successfully to produce nanoparticles.<sup>49</sup> Pulsed laser ablation in liquid (PLAL) method gives permission to produce versatile NPs and this technique compared to chemical methods known as a green synthesized method with minimum chemicals.<sup>50,51</sup> PLAL is a powerful technique for production of NPs experimentally. Compared to other physical procedures, PLAL is particularly common because of its unique characteristics such as being rapid and simple, not requiring the use of hazardous chemicals, producing long-term stable dispersions, and being performed at room temperature. It is a very appealing approach, especially because it can be conducted on a variety of targets in a variety of solvents and delivers great purity due to the incidence of a direct laser beam on the target. In recent years, nanomembranes with new

properties can be produced with the integration of the green laser ablation process into the electrospinning technique, and these nanofibrous membranes have attracted the attention of researchers in many application areas, including antibacterial materials,<sup>52</sup> wound healing,<sup>53</sup> tissue engineering,<sup>54</sup> photocatalysis,<sup>55</sup> dye<sup>56</sup> and phosphate removal.<sup>56</sup> However, when similar studies are examined, it is seen that there is a gap in the literature regarding the application to oil-water separation of nanofibrous membranes prepared by incorporating nanoparticles produced by laser ablation to the electrospinning solution.

In earlier research, petro-based polymers commonly employed for manufacturing membrane materials frequently scarcely decomposed in the nature. Thus, usage of these polymers for removal of oil from water in oil-water mixture may result in secondary contamination. Furthermore, the unpredictability of crude oil prices, the depletion of petroleum supplies, and the negative environmental effects of petroleum-based polymers continue to be the main concerns. For this, an innovative sustainable strategy in membrane production is to use biodegradable polymers that can deteriorate in natural conditions. Various eco-friendly bio-based polymers have used to produce nanofiber membranes for oil-water separation, such as polycaprolactone (PCL),<sup>41</sup> polylactic acid,<sup>57</sup> chitosan,<sup>58</sup> cellulose<sup>59</sup> and polyhydroxybutyrate.<sup>38</sup> Among these bio-based polymers, poly(3)-hydroxybutyrate (PHB) with outstanding properties such as biodegradability and biocompatibility are regarded as one of the most promising ecologically friendly biomaterials for preparing membrane materials in various fields.<sup>60–62</sup> PHB's non-toxicity, mechanical strength, relatively high melting point, ease of blending with various polymers, and solubility in a wide variety of solvents make it an attractive supply for applications in the medical, agricultural and industrial fields.<sup>30</sup> In some previously published studies, PHB/PLA nanofiber mats have been produced by electrospinning method by preparing blends of PHB with polylactic acid for selective sorption of oil from aqueous media, and successful results were obtained.<sup>38,63</sup>

In this work, hydrophobic SiO<sub>2</sub> NPs were selected as the modifying materials to increase the surface roughness and adjust the surface wettability behavior of PHB nanofibers. PHB polymer is employed as a matrix for fabrication of a bionanofiber membrane because PHB is an eco-friendly polymer. This study aims to demonstrate the fabrication of superhydrophobic-superoleophilic PHB-SiO<sub>2</sub> bionanofiber membranes for effective separation of oil and water. For the first time, PHB-SiO<sub>2</sub> bio-based nanofiber mats obtained on stainless steel meshes by adding silica nanoparticles produced by laser ablation method to the PHB solution using electrospinning method were applied to oil-water separation. Hydrophobic SiO<sub>2</sub> NPs were loaded into PHB work solution to produce SH-SO bio-nanofiber membrane. By altering laser ablation time,

the content of SiO<sub>2</sub> NPs added into spinning solution was adjusted to control the surface energy and roughness of nanofibers and then morphology, chemical structure, and wetting properties of nanofibrous mats coated on the stainless-steel mesh surface having various sizes of mesh used as collector has been investigated. After electrospun PHB-SiO<sub>2</sub> nanofibrous mats were applied to the stainless steel meshes, they became superhydrophobic and superoleophilic, allowing an efficient separation of oil and water. The prepared SH and SO PHB-SiO<sub>2</sub> bio-nanofiber membranes were directly employed for gravity-driven separation of oil and water.

## 2 | EXPERIMENTAL

### 2.1 | Materials

Polyhydroxybutyrate granules (PHB, Mw = 500 kDa, Aldrich), silicon dioxide pieces (SiO<sub>2</sub>, 99,99%, Lesker), *N*-dimethylformamide (DMF, 99,8%, Aldrich), chloroform (CF, 99%, Aldrich), ethanol (Eth, 96%, Aldrich) and acetone (Ac, 98%, Aldrich) were obtained commercially. Stainless steel meshes having different pore diameters (283, 106, 61 and 34 μm) were provided from Cromtel in Turkey. All of chemicals had analytical grade and were used as purchased. All nanofibrous mats were produced using an electrospinning device by courtesy of Laser Spectroscopy Group (LSG) at Physics Department, Selcuk University.

### 2.2 | Synthesis of silica NPs by femtosecond laser ablation method

Silica NPs have been prepared using femtosecond (fs) micromachining unit with Ti: Sapphire crystal which this laser system has promising properties to produce NPs. This fs laser system has features that allow the user to change laser parameters such as pulse repetition rate, laser wavelength and laser pulse energy.<sup>64</sup> Fs laser system with Ti: Sapphire crystal has delivered an output beam at 90 fs laser pulse duration, the fundamental wavelength of beam at 800 nm and the repetition rate can be changeable 1–3 kHz at 3.5 W laser pulse power (Quantronix, NY, USA).<sup>65</sup> Experimental setup is shown in Figure 1a which Si pellets were placed in DMF solvent. This technique is known as classical PLAL method which gives opportunities to produce new NPs based technologies as green synthesized with rapid and minimum chemicals.<sup>66</sup> In this study, Si pellets were placed in a container. Fs laser was focused using 11 cm F-theta lens on Si pellets about 30 min in micromachining unit which is used as laser unit to control the machining parameters on targets.<sup>67</sup>

### 2.3 | Preparation of electrospun PHB-SiO<sub>2</sub> nanofibrous mats

Firstly, commercial stainless-steel meshes with various pore diameters were cut (4 × 4 cm). Later, these meshes were treated in an ultrasonicator with ethanol, acetone and distilled water for 15 min, respectively. The sterilized meshes were held in an oven at 60°C for 60 min for completely removing the solvents. In order to produce PHB nanofibrous mat, PHB granules (0.90 g) were dissolved in a 10 ml mixture of CF and 1.25 ml DMF (v/v, 8:1) and 5% (w/v) PHB/CF-DMF solution was constantly stirred at 50°C for 1 h in order to obtain a homogeneous mixture. Respectively, for fabricating PHB-SiO<sub>2</sub>(1), PHB-SiO<sub>2</sub>(2) and PHB-SiO<sub>2</sub>(3) composite nanofibers, the pure PHB was dissolved in 10 ml of CF solvent and the prepared PHB solution was magnetically stirred for the time and at the temperature needed for complete dissolution, and then SiNPs (in DMF solvent (1,25 ml)) synthesized by laser ablation at the different time (15, 30 and 60 min) were loaded into the prepared PHB solutions. All the solutions were further stirred magnetically at ambient temperature for 30 min. The spinning solutions were added into a 10 ml plastic syringe fitted with a 20-G needle and later electrospinning process was performed at a range of optimal parameters, including: supplied high voltage, 18 kV; distance from the needle tip to the collector, 12 cm; flow rate, 4 ml/h; temperature (T), 35 C; and relative humidity (RH), 40%. The resulting fibrous mats were gathered on aluminum foil and the mesh substrates enwrapped by a rolling drum. In order to remove the solvent residue, the obtained samples were subsequently dried overnight in an oven at 50°C. Schematic illustration of SiNPs synthesis and production processes of PHB-SiO<sub>2</sub> bionanofiber membrane is given in Figure 1.

### 2.4 | Gravity-driven oil and water separation setup

The efficiency of oil and water separation was tested with a gravity-driven separation device as described in literature.<sup>68</sup> The performance of oil and water separation of PHB-SiO<sub>2</sub> bionanofiber membranes was investigated by the separation of oil and water mixture. For this purpose, a mixture of oil (diesel) and water in equal amounts was poured onto PHB-SiO<sub>2</sub> nanofiber coated stainless steel mesh surfaces. All PHB-SiO<sub>2</sub> nanofiber membranes were sloped at a 45° angle to allow oil (diesel) to pass directly over the mesh surface while water rolled off, oil and water amount collected in two different vessels were recorded. To visually examine the separation of the water and oil mixture, the water was colored with red food coloring. The volumes of oil and water collected in separate beakers utilizing sloped

bionanofiber membranes were used to calculate the oil and water separation efficiency. For this, the amount of oil pre and post separation was weighed, and according to Equation (1), the separation efficiency  $E$  was calculated.

$$E = \frac{M_1}{M_0} \times 100\% \quad (1)$$

where  $M_0$  and  $M_1$  represent the weight of oil before and after separation. The data was presented as average SD ( $n = 5$ )<sup>69</sup>.

## 2.5 | Material characterization

The chemical structure of the fabricated nanofibrous mats was investigated in the spectral range of 400–4000  $\text{cm}^{-1}$  at 4  $\text{cm}^{-1}$  resolution by Fourier Transform Infrared spectroscopy (FT-IR; Thermo Scientific-Nicolet iS20) and the surface morphologies of the prepared bionanofiber membranes were evaluated using Field Emission Scanning Electron microscopy (FE-SEM; Zeiss GeminiSEM 500) and High-resolution Transmission

Electron microscopy (HR-TEM; Jeol-Jem 2100). Diameters of the produced PHB and PHB-SiO<sub>2</sub> nanofibers were also determined from images FE-SEM. The water contact angle (WCA) and oil contact angle (OCA) of bionanofiber

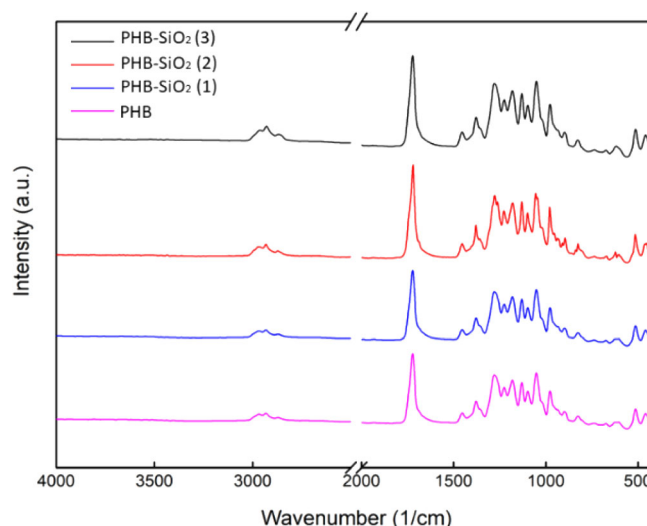


FIGURE 3 FTIR spectra of the PHB and PHB-SiO<sub>2</sub> samples [Color figure can be viewed at [wileyonlinelibrary.com](https://onlinelibrary.wiley.com/doi/10.1002/app.53542)]

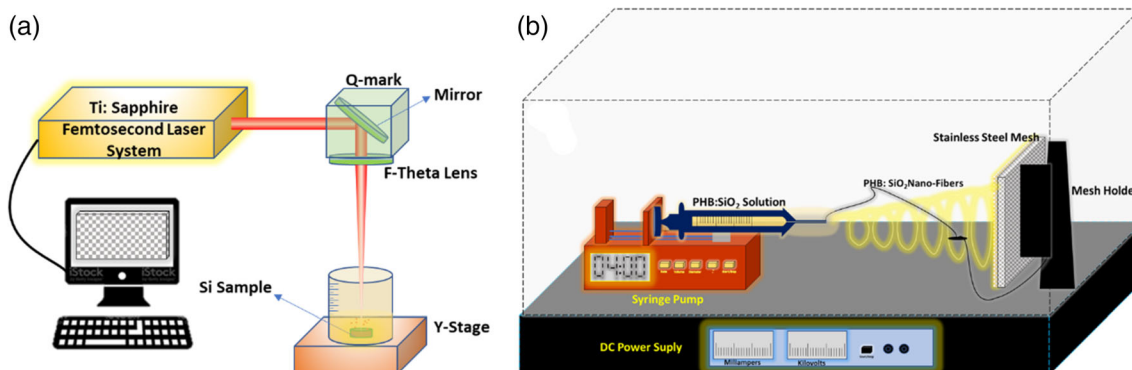


FIGURE 1 Schematic illustration of (a) laser ablation based SiNPs synthesis and (b) production processes of PHB-SiO<sub>2</sub> bionanofiber membrane in electrospinning system. [Color figure can be viewed at [wileyonlinelibrary.com](https://onlinelibrary.wiley.com/doi/10.1002/app.53542)]

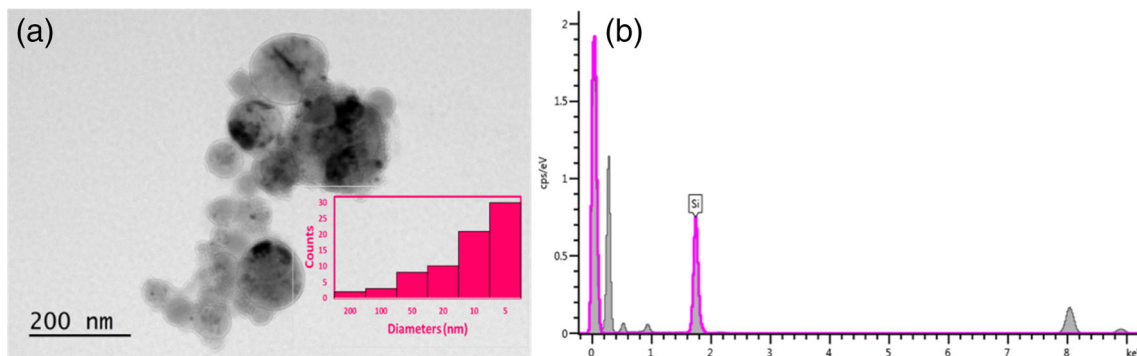


FIGURE 2 (a) TEM and (b) TEM-EDS images of SiNPs prepared using fs laser ablation<sup>65</sup> [Color figure can be viewed at [wileyonlinelibrary.com](https://onlinelibrary.wiley.com/doi/10.1002/app.53542)]

membrane surfaces were measured with a contact angle goniometer at room temperature. For contact angle testing, drops of distilled water in a volume of 4  $\mu\text{l}$  were dropped onto each membrane surface at ambient temperature. Contact angle value of all samples were obtained by averaging over five individual measurements.

### 3 | RESULT AND DISCUSSION

#### 3.1 | Characterization of synthesized SiNPs

In this work, laser ablation based SiNPs synthesizing has been carried out by running fs laser system with an

**TABLE 1** Composition of PHB and its composite nanofibers corresponding to different laser ablation times

Sample	Laser ablation time (min)	Content of PHB and SiO <sub>2</sub> NPs (%w/v)
PHB	0	6:0
PHB-SiO <sub>2</sub> (1)	15	6:0.01
PHB-SiO <sub>2</sub> (2)	30	6:0.02
PHB-SiO <sub>2</sub> (3)	60	6:0.03

output at a wavelength of 800 nm, about 30 min irradiation time and applying 350 mW laser power. It has been obtained that the size distribution of NPs was observed between 5 nm and 200 nm with spherical shape for SiNPs in DMF solution as shown in Figure 2a and TEM-EDS represents fairly well peaks with pure silica EDS peaks as shown in Figure 2b.

#### 3.2 | Chemical structure and morphology of PHB-SiO<sub>2</sub> nanofibrous mats

The chemical structure of nanofibrous mats obtained was analyzed using FT-IR spectroscopy. FT-IR spectra of PHB fibrous mat and PHB-SiO<sub>2</sub> nanocomposite fibrous mats with different SiNPs content (PHB-SiO<sub>2</sub>(1), PHB-SiO<sub>2</sub>(2) and PHB-SiO<sub>2</sub>(3)) were shown in Figure 3. SiO<sub>2</sub> NPs nanoparticle contents corresponding to different laser ablation times for each nanofiber sample are given in Table 1. In the spectrum of PHB nanofibers, C=O stretching vibrations at 1720  $\text{cm}^{-1}$ ; asymmetric  $-\text{CH}_3$  at 1456  $\text{cm}^{-1}$ ; symmetrical  $-\text{CH}_3$  at 1379  $\text{cm}^{-1}$ ; C-O-C stretch at 1276  $\text{cm}^{-1}$ , 1228  $\text{cm}^{-1}$  and 1180  $\text{cm}^{-1}$ ; C-O-C stretch at 1261  $\text{cm}^{-1}$ ; C-O stretch at 1055  $\text{cm}^{-1}$ ; and C-CH<sub>3</sub> stretch at 1043  $\text{cm}^{-1}$  were observed, respectively.<sup>70</sup> When FTIR spectrum of PHB-SiO<sub>2</sub> nanocomposite fibrous mats was

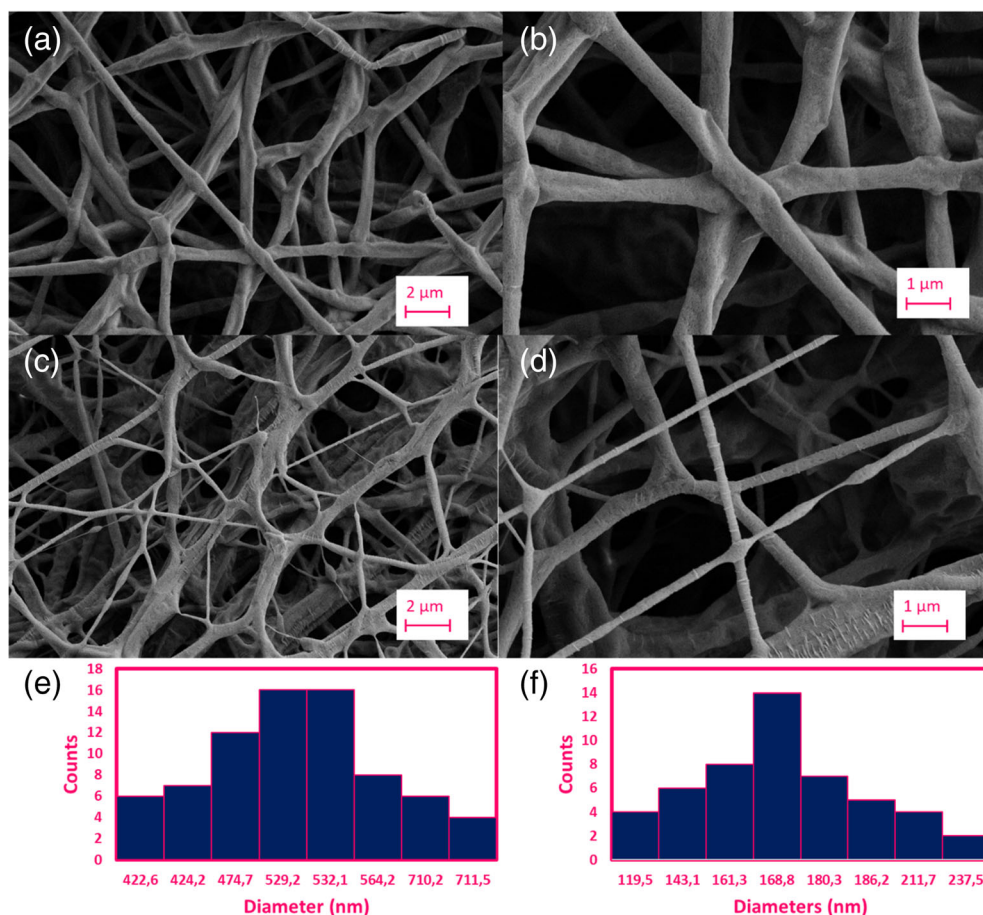


**FIGURE 4** FE-SEM images of PHB nanofibers with (a) 2  $\mu\text{m}$ , (b) 1  $\mu\text{m}$  size distribution, and PHB-SiO<sub>2</sub> (3) nanofibers (c) 2  $\mu\text{m}$ , (d) 1  $\mu\text{m}$  size distribution and the histograms of the fiber size distribution of (e) PHB and (f) PHB-SiO<sub>2</sub>(3) fibrous mats. [Color figure can be viewed at [wileyonlinelibrary.com](http://wileyonlinelibrary.com)]

investigated, no significant difference was observed compared to the spectrum of PHB. The characteristic adsorption peaks at 1197 and 1083  $\text{cm}^{-1}$  are attributed to the asymmetrical stretching vibration of Si—O—Si groups. When compared to spectra of PHB and other composite nanofibrous samples in Figure 3, some slightly shifts in peaks were observed because of an interaction of silica with PHB. The increase in peak intensity with an increase in SiNPs content could be because of the creation of new bonds and/or atoms in the medium, which resulted in a decline in the frequencies of nanocomposite fibers towards less frequency values in comparison with pure PHB fibers.<sup>71</sup>

The surface morphology and diameter distributions of the prepared nanofiber mats were observed by FE-SEM and given in Figure 4. All nanofibers have exhibited continuous nanostructures without bead formation, and due to the hydrophobic nature of PHB and SiNPs with low surface energy, rough structures of both pure PHB and PHB-SiO<sub>2</sub> nanofibers were clearly seen from pictures. The mean fiber diameters of PHB and PHB-SiO<sub>2</sub> nanofibers were determined as between 422.6 nm and 711.5 nm as well as between 119.5 nm and 237.5 nm, and the histograms of fiber size distribution were given in Figure 4c,f, respectively. It was detected that there was a decrease in fiber diameter sizes as SiNPs were added to PHB nanofibers. This difference could be due to decreased viscosity and higher conductivity of PHB-SiO<sub>2</sub> solution compared to PHB solution. One of the most critical electrospinning parameters affecting fiber diameter is solution viscosity. A solution with a higher viscosity produces fibers with higher diameters, whereas a solution with a lower viscosity produces fibers with smaller diameters, and excess even results in the formation of beads.

### 3.3 | Wetting properties of the prepared PHB-SiO<sub>2</sub> bionanofiber membranes

The wettability of surfaces is a key factor affecting the separation performance of an oil–water mixture. The incorporation of silica particles to PHB nanofibers enhanced their roughness, which could influence their wettability. The contact angle of water and oil in air was measured to investigate the effect of SiO<sub>2</sub> content and mesh size on the wettability of PHB nanofibrous membrane (shown in Figure 5). Because the uncoated stainless steel meshes was of oleophilic-hydrophilic structure, they were wetted with oil and water quickly and easily. Both oil and water went through the uncoated mesh with PHB-SiO<sub>2</sub> without any difficulty. The coated meshes with PHB-SiO<sub>2</sub> nanofibers, on the other hand, showed diverse wetting tendencies towards oil and water. PHB-SiO<sub>2</sub>

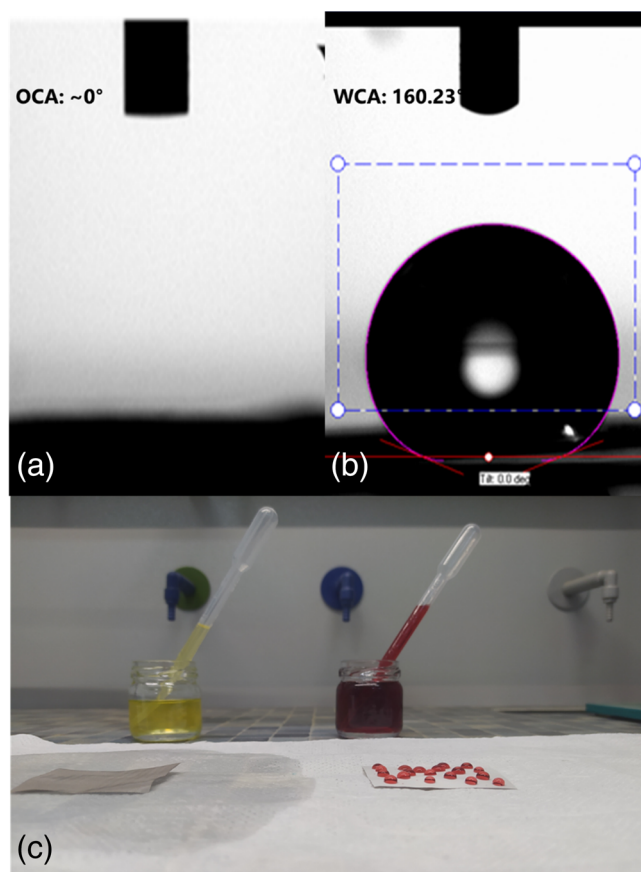


**FIGURE 5** (a) OCA ( $\sim 0^\circ$ ) and (b) WCA ( $160.23^\circ$ ) of electrospun PHB-SiO<sub>2</sub>(3) nanofibrous mats on stainless steel mesh; and (c) photographs of diesel oil (on the left) and water (on the right) drops on the coated mesh PHB-SiO<sub>2</sub>(3) nanofibrous mat [Color figure can be viewed at [wileyonlinelibrary.com](https://onlinelibrary.wiley.com/doi/10.1002/app.53542)]

bionanofiber membrane had a water and oil contact angle of  $160.23^\circ$  and  $0^\circ$ , respectively, demonstrating the high hydrophobicity and oleophilicity (as seen from Figure 5).

The influence of SiNPs content and mesh size on the wetting properties of PHB-SiO<sub>2</sub> nanofibrous membranes has been thoroughly studied in this work. In Figure 6, the alterations in water contact angle (WCA) values as a function of SiNPs content and mesh size have been given. WCA values greater than  $130^\circ$  were measured on all membrane surfaces. It was observed that the WCA values of the membrane surfaces increased as the SiO<sub>2</sub> NPs content increased. This increase in WCA value occurs due to the additional roughness of the macrostructure of the mesh itself, and also the introduction of extra air beneath the drop.<sup>72</sup> The alterations in WCA values, rather than mesh pore diameters, were of more significant in terms of SiNPs contents. It was observed that WCA values for PHB-SiO<sub>2</sub> nanofiber membranes slightly increased with increasing mesh size. The highest WCA value was detected for the sample with a mesh size of 106  $\mu\text{m}$ .

When the surface morphologies of the 106 and 283  $\mu\text{m}$  sized meshes are compared, it could be concluded that the formed morphologies on the meshes with pore size of 106  $\mu\text{m}$  are more uniform and therefore less irregularity can be seen. So for the 106  $\mu\text{m}$  pore size mesh, it may be the fact that a higher surface area of the mesh encounters the polymer/nanoparticle suspension. On such a mesh surface, PHB-SiO<sub>2</sub>(3) nanofibrous mats has exhibited a superhydrophobic surface having a WCA value of 160.23°. It's worth noting that all mesh surfaces coated with PHB-SiO<sub>2</sub>(3) nanofibrous mats has displayed superoleophilic property with OCA of 0°.

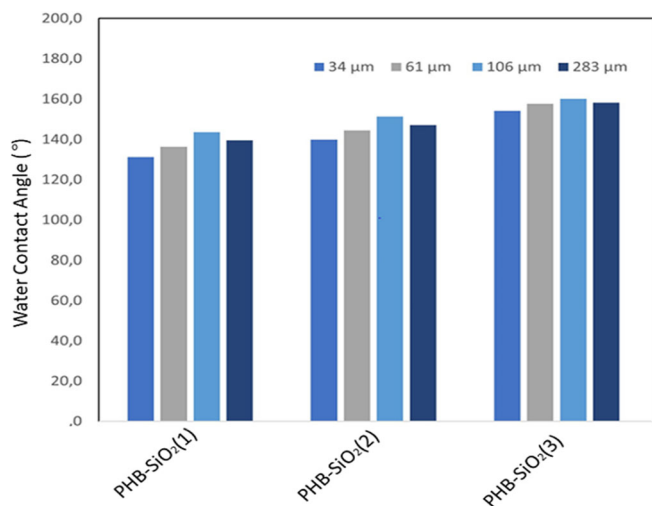


**FIGURE 6** The relationship between the mesh sizes and the WCA on the PHB-SiO<sub>2</sub> bionanofiber membranes with various SiNPs content ( $n = 5$ ) [Color figure can be viewed at [wileyonlinelibrary.com](https://onlinelibrary.wiley.com)]

### 3.4 | Oil-water separation

The oil-water separation was performed by employing a gravity-driven separation device, which did not require any additional force or chemical reagents. Non-coated and PHB-SiO<sub>2</sub> nanofiber coated meshes were placed over the beakers and then the shaken oil-water mixture was poured over them. It was seen that the uncoated mesh quickly passed the oil-water mixture with no separation. However, the oil component was permeated by PHB-SiO<sub>2</sub> nanofiber membrane, while the water component remained suspended on its surface (as shown in Figure 7a). Later, the membrane was sloped at an angle of 45° and the separation was carried out by pouring the shaken oil-water mixture onto PHB-SiO<sub>2</sub> nanofiber membranes. The slope of meshes was necessitated to let water separated by rolling from the membrane surface to flow into an adjacent vessel, where gravity is the only driving force for separation. As a result, it was detected that the water contained no visible oil (Figure 7b-c). Therefore, utilizing only the weights of the liquids and no additional force or chemical reagents, the oil-water mixture was successfully separated with a gravity-driven simple experimental setup. The separation efficiency of PHB-SiO<sub>2</sub>(3) nanofiber coated mesh (with pore size of 106  $\mu\text{m}$ ) was determined to be 99.4%.

## 4 | CONCLUSIONS

Superhydrophobic and super-oleophilic poly(3)-hydroxybutyrate-SiO<sub>2</sub> bionanofiber membranes were successfully fabricated by combination of electrospinning and green

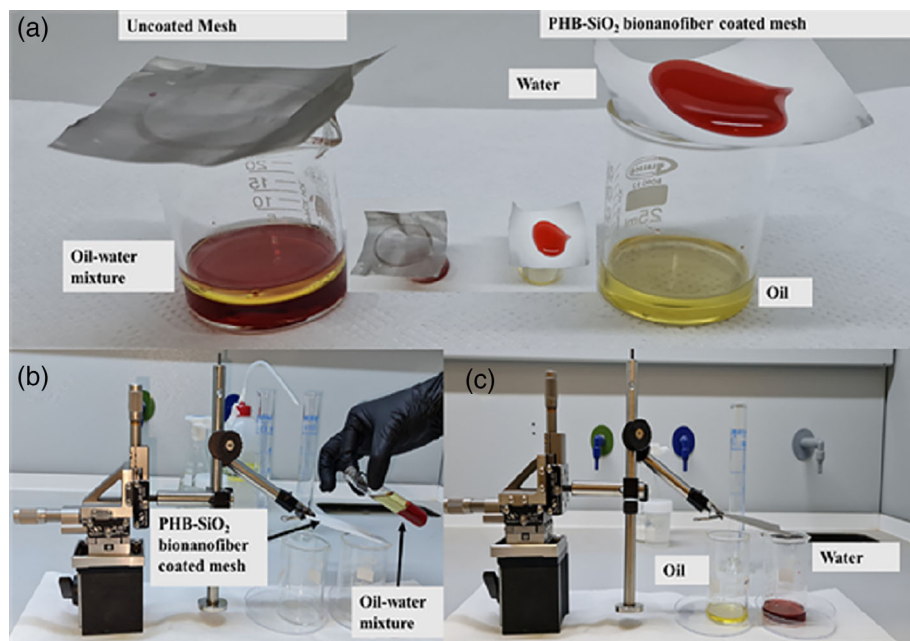


**FIGURE 7** Illustration of separation of oil-water mixture: (a) shaken oil-water mixture poured on PHB-SiO<sub>2</sub>(3) nanofibrous mat coated and uncoated meshes; (b), (c) dispersion of mixture of oil and water on PHB-SiO<sub>2</sub> bionanofiber membrane inclined at 45° for gravity-driven continuously separation [Color figure can be viewed at [wileyonlinelibrary.com](https://onlinelibrary.wiley.com)]



laser ablation techniques. The maximum the water contact angle value obtained after the production of PHB-SiO<sub>2</sub>(3) nanofibrous mats on stainless steel meshes was 160.23°, and the oil contact angle value was measured to be close to zero. Electrospinning-modified mesh surfaces behaved as a membrane separating diesel oil and water with a separation efficiency of 99.4%. These results have shown that meshes modified with such eco-friendly poly(3)-hydroxybutyrate-SiO<sub>2</sub> biocomposite nanofibers and could be considered to be a promising membrane material for oil–water separation application in various fields.

## AUTHOR CONTRIBUTIONS

**Fatma Bayram Sariipek:** Conceptualization (equal); formal analysis (equal); investigation (equal); methodology (equal); software (equal); visualization (lead); writing – original draft (equal); writing – review and editing (equal). **Yasemin Gündoğdu:** Conceptualization (equal); formal analysis (equal); investigation (equal); resources (lead); visualization (lead); writing – original draft (equal); writing – review and editing (equal). **Hamdi Şükür Kiliç:** Conceptualization (equal); formal analysis (lead); investigation (equal); project administration (lead); supervision (lead); writing – original draft (lead); writing – review and editing (lead).

## ACKNOWLEDGMENTS

Author kindly would like to thank Selçuk University for:  
 - High Technology Research and Application Center (İL-TEK) and SULTAN Center for infrastructures.  
 - Selcuk University Scientific Research Project (BAP) Coordination for the support with the project number of 19401140.


## DATA AVAILABILITY STATEMENT

Research data are not shared.

## ORCID

Fatma Bayram Sariipek  <https://orcid.org/0000-0001-8168-3517>

Yasemin Gündoğdu  <https://orcid.org/0000-0003-2020-9533>

Hamdi Şükür Kiliç  <https://orcid.org/0000-0002-7546-4243>

## REFERENCES

- [1] J. Ge, H. Y. Zhao, H. W. Zhu, J. Huang, L. A. Shi, S. H. Yu, *Adv. Mater.* **2016**, *28*, 10459.
- [2] L. Qiu, Y. Sun, Z. Guo, *J. Mater. Chem. A* **2020**, *8*, 16831.
- [3] W. Kang, Y. Cui, L. Qin, Y. Yang, Z. Zhao, X. Wang, X. Liu, *J. Hazard. Mater.* **2020**, *392*, 122499.
- [4] A. Abidli, Y. Huang, P. Cherukupally, A. M. Bilton, C. B. Park, *Environ. Technol. Innov.* **2020**, *18*, 100598.
- [5] F. C. P. Rocha e Silva, N. M. P. Rocha e Silva, J. M. Luna, R. D. Rufino, V. A. Santos, L. A. Sarubbo, *Rev. Environ. Sci. Bio/Technol.* **2018**, *17*, 591.
- [6] N. Khatri, J. Andrade, E. Baydak, H. Yarranton, *Colloids Surf., A* **2011**, *384*, 630.
- [7] K. T. Klasson, P. A. Taylor, J. F. Walker Jr., S. A. Jones, R. L. Cummins, S. A. Richardson, *Sep. Sci. Technol.* **2005**, *40*, 453.
- [8] Y. Zeng, C. Yang, J. Zhang, W. Pu, *J. Hazard. Mater.* **2007**, *147*, 991.
- [9] Y. Liu, C.-H. Choi, *Colloid Polym. Sci.* **2013**, *291*, 437.
- [10] Y. Sun, Z. Guo, *Nanoscale Horiz.* **2019**, *4*, 52.
- [11] J. Liu, P. Li, L. Chen, Y. Feng, W. He, X. Yan, X. Lü, *Surf. Coat. Technol.* **2016**, *307*, 171.
- [12] S. M. S. Shahabadi, J. A. Brant, *Sep. Purif. Technol.* **2019**, *210*, 587.
- [13] G. J. Dunderdale, M. W. England, T. Sato, C. Urata, A. Hozumi, *Macromol. Mater. Eng.* **2016**, *301*, 1032.
- [14] Y. Sun, Z. Guo, *Adv. Mater.* **2020**, *32*, 2004875.
- [15] M. Ma, Y. Mao, M. Gupta, K. K. Gleason, G. C. Rutledge, *Macromolecules* **2005**, *38*, 9742.
- [16] S. Michielsen, H. J. Lee, *Langmuir* **2007**, *23*, 6004.
- [17] J. Usman, M. H. D. Othman, A. F. Ismail, M. A. Rahman, J. Jaafar, Y. O. Raji, A. O. Gbadamosi, T. H. El Badawy, K. A. M. Said, *J. Mater. Res. Technol.* **2021**, *12*, 643.
- [18] C.-T. Liu, P.-K. Su, C.-C. Hu, J.-Y. Lai, Y.-L. Liu, *J. Membr. Sci.* **2018**, *546*, 100.
- [19] M. Zhu, Y. Liu, M. Chen, Z. Xu, L. Li, Y. Zhou, *J. Pet. Sci. Eng.* **2021**, *205*, 108889.
- [20] M. Padaki, R. S. Murali, M. S. Abdullah, N. Misdan, A. Moslehyani, M. Kassim, N. Hilal, A. Ismail, *Desalination* **2015**, *357*, 197.
- [21] R. K. Gupta, G. J. Dunderdale, M. W. England, A. Hozumi, *J. Mater. Chem. A* **2017**, *5*, 16025.
- [22] M. Wang, M. Peng, J. Zhu, Y.-D. Li, J.-B. Zeng, *Carbohydr. Polym.* **2020**, *244*, 116449.
- [23] J.-J. Li, Y.-N. Zhou, Z.-H. Luo, *Prog. Polym. Sci.* **2018**, *87*, 1.
- [24] S. Han, Q. Song, X. Feng, J. Wang, X. Zhang, Y. Zhang, *ACS Appl. Nano Mater.* **2021**, *4*, 11809.
- [25] F. Z. Pour, H. Karimi, V. M. Avargani, *Polyhedron* **2019**, *159*, 54.
- [26] M. W. Lee, S. An, S. S. Latthe, C. Lee, S. Hong, S. S. Yoon, *ACS Appl. Mater. Interfaces* **2013**, *5*, 10597.
- [27] X. Yin, S. Yu, L. Wang, J. Wang, B. Wang, H. Li, Z. Chen, *Surf. Coat. Technol.* **2022**, *434*, 128177.
- [28] S. Rasouli, N. Rezaei, H. Hamed, S. Zendejboudi, X. Duan, *Chem. Eng. Sci.* **2021**, *236*, 116354.
- [29] D. Guo, K. Hou, S. Xu, Y. Lin, L. Li, X. Wen, P. Pi, *J. Mater. Sci.* **2018**, *53*, 6403.
- [30] H. Yang, P. Pi, Z.-Q. Cai, X. Wen, X. Wang, J. Cheng, Z.-r. Yang, *Appl. Surf. Sci.* **2010**, *256*, 4095.
- [31] A. Huang, C.-C. Kan, S.-C. Lo, L.-H. Chen, D.-Y. Su, J. F. Soesanto, C.-C. Hsu, F.-Y. Tsai, K.-L. Tung, *J. Membr. Sci.* **2019**, *582*, 120.
- [32] X. Li, D. Hu, K. Huang, C. Yang, *J. Mater. Chem. A* **2014**, *2*, 11830.
- [33] F. Bayram, E. S. Mercan, M. Karaman, *Colloid Polym. Sci.* **2021**, *299*, 1469.
- [34] Z. Huang, Y. Liu, W. He, W. Tu, M. Chen, M. Zhu, R. Liu, *Colloids Surf., A* **2022**, *635*, 127938.
- [35] R. Su, S. Li, W. Wu, C. Song, G. Liu, Y. Yu, *Sep. Purif. Technol.* **2021**, *256*, 117790.

- [36] J. Wu, Y. Ding, J. Wang, T. Li, H. Lin, J. Wang, F. Liu, *J. Mater. Chem. A* **2018**, *6*, 7014.
- [37] S. M. Moatmed, M. H. Khedr, S. El-Dek, H.-Y. Kim, A. G. El-Deen, *J. Environ. Chem. Eng.* **2019**, *7*, 103508.
- [38] J. C. C. Yeo, D. Kai, C. P. Teng, E. M. J. R. Lin, B. H. Tan, Z. Li, C. He, *ACS Appl. Polym. Mater.* **2020**, *2*, 4825.
- [39] S. Jiang, X. Meng, B. Chen, N. Wang, G. Chen, *J. Appl. Polym. Sci.* **2020**, *137*, 49546.
- [40] Y. Yang, Y. Li, L. Cao, Y. Wang, L. Li, W. Li, *Sep. Purif. Technol.* **2021**, *269*, 118726.
- [41] X. Zhang, J. Zhao, L. Ma, X. Shi, L. Li, *J. Mater. Chem. A* **2019**, *7*, 24532.
- [42] M. Obaid, G. M. Tolba, M. Motlak, O. A. Fadali, K. A. Khalil, A. A. Almajid, B. Kim, N. A. Barakat, *Chem. Eng. J.* **2015**, *279*, 631.
- [43] L.-Y. Yu, Z.-L. Xu, H.-M. Shen, H. Yang, *J. Membr. Sci.* **2009**, *337*, 257.
- [44] F. Ardeshiri, A. Akbari, M. Peyravi, M. Jahanshahi, *Korean J. Chem. Eng.* **2019**, *36*, 255.
- [45] Y. Zhou, X. Wu, X. Zhong, W. Sun, H. Pu, J. X. Zhao, *ACS Appl. Mater. Interfaces* **2019**, *11*, 45763.
- [46] X. Lin, S. Li, J. Jung, W. Ma, L. Li, X. Ren, Y. Sun, T.-S. Huang, *RSC Adv.* **2019**, *9*, 23071.
- [47] Z.-Y. Ying, Z.-D. Shao, L. Wang, X. Cheng, Y.-M. Zheng, *J. Mater. Sci.* **2020**, *55*, 16129.
- [48] F. E. Kruis, H. Fissan, A. Peled, *J. Aerosol Sci.* **1998**, *29*, 511.
- [49] L. Krishnia, P. Thakur, A. Thakur, *In Synthesis and Applications of Nanoparticles*, Springer, Singapore **2022**, pp. 45–59.
- [50] R. Kuladeep, L. Jyothi, C. Sahoo, D. Narayana Rao, V. Saikiran, *J. Mater. Sci.* **2022**, *57*, 1863.
- [51] S.-y. Liang, Y. Yang, J.-h. Zhao, H. Xia, *Measurement* **2022**, *198*, 111364.
- [52] D. A. Goncharova, E. N. Bolbasov, A. L. Nemyokina, A. A. Aljulaih, T. S. Tverdokhlebova, S. A. Kulinich, V. A. Svetlichnyi, *Materials* **2020**, *14*, 2.
- [53] I. V. Lukiev, L. S. Antipina, S. I. Goreninskii, T. S. Tverdokhlebova, D. V. Vasilchenko, A. L. Nemyokina, D. A. Goncharova, V. A. Svetlichnyi, G. T. Dambaev, V. M. Bouznic, *Membranes* **2021**, *11*, 986.
- [54] A. Al-Kattan, V. P. Nirwan, E. Munnier, I. Chourpa, A. Fahmi, A. V. Kabashin, *RSC Adv.* **2017**, *7*, 31759.
- [55] A. Menazea, H. M. Assaggaf, S. Alghamdi, E. H. Eldrehmy, M. T. Elabbasy, A. El-Kader, *J. Mater. Sci.: Mater. Electron.* **2022**, *33*, 1021.
- [56] M. Ahmed, M. E. El-Naggar, K. Mahmoud, F. M. Abdel-Rahim, A. Menazea, *J. Polym. Res.* **2021**, *28*, 1.
- [57] L. Liu, W. Yuan, *New J. Chem.* **2018**, *42*, 17615.
- [58] H. N. Doan, P. P. Vo, A. Baggio, M. Negoro, K. Kinashi, Y. Fuse, W. Sakai, N. Tsutsumi, *ACS Appl. Polym. Mater.* **2021**, *3*, 3891.
- [59] M. Zhang, S. Jiang, F. Han, M. Li, N. Wang, L. Liu, *Carbohydr. Polym.* **2021**, *264*, 118033.
- [60] J. Guo, Q. Zhang, Z. Cai, K. Zhao, *Sep. Purif. Technol.* **2016**, *161*, 69.
- [61] A. Nicosia, W. Gieparda, J. Foksowicz-Flaczyk, J. Walentowska, D. Wesotek, B. Vazquez, F. Prodi, F. Belosi, *Sep. Purif. Technol.* **2015**, *154*, 154.
- [62] A. Venault, A. Subarja, Y. Chang, *Langmuir* **2017**, *33*, 2460.
- [63] A. Iordanskii, N. Samoilov, A. Olkhov, V. Markin, S. Rogovina, N. Kildeeva, A. Berlin, *Dokl. Phys. Chem.* **2019**, *487*, 106.
- [64] V. Vendamani, S. Hamad, V. Saikiran, A. Pathak, S. Venugopal Rao, V. Ravi Kanth Kumar, S. Nageswara Rao, *J. Mater. Sci.* **2015**, *50*, 1666.
- [65] Y. Gündoğdu, A. Kepceoğlu, S. Y. Gezgin, H. Küçükçelebi, H. Ş. Kiliç, *Mater. Today: Proc.* **2019**, *18*, 1803.
- [66] A. Y. Vorobyev, C. Guo, *Laser Photonics Rev.* **2013**, *7*, 385.
- [67] A. Kepceoğlu, Y. Gündoğdu, A. Sarilmaz, M. Ersöz, F. Özel, H. Ş. Kiliç, *Turk. J. Chem.* **2021**, *45*, 485.
- [68] P. Brown, O. Atkinson, J. Badyal, *ACS Appl. Mater. Interfaces* **2014**, *6*, 7504.
- [69] Q. Pan, M. Wang, H. Wang, *Appl. Surf. Sci.* **2008**, *254*, 6002.
- [70] T. Furukawa, H. Sato, R. Murakami, J. Zhang, Y.-X. Duan, I. Noda, S. Ochiai, Y. Ozaki, *Macromolecules* **2005**, *38*, 6445.
- [71] S. Gu, J. Zhou, Z. Luo, Q. Wang, M. Ni, *Ind. Crops Prod.* **2013**, *50*, 540.
- [72] B. Deng, R. Cai, Y. Yu, H. Jiang, C. Wang, J. Li, L. Li, M. Yu, J. Li, L. Xie, *Adv. Mater.* **2010**, *22*, 5473.

**How to cite this article:** F. B. Sariipek, Y. Gündoğdu, H. Ş. Kiliç, *J. Appl. Polym. Sci.* **2023**, *140*(9), e53542. <https://doi.org/10.1002/app.53542>